Fermi National Accelerator Laboratory

FERMILAB-PUB-91/187-T

July 1991

CLASS OF MODELS LEADING TO DEPLETIONS OF SOLAR ν_e AND ATMOSPHERIC ν_μ NEUTRINO FLUXES

Carl H. ALBRIGHT

Department of Physics, Northern Illinois University, DeKalb, Illinois 60115*

and

Fermi National Accelerator Laboratory, P.O. Box 500, Batavia, Illinois 60510†

Abstract

A model incorporating three lefthanded $SU(2)_L \times U(1)_Y$ doublet neutrinos and three righthanded singlet neutrinos, with leptonic Dirac mass submatrices similar to empirical forms which work well for quarks, is required to yield both the nonadiabatic MSW solar neutrino effect and the depleted flux of atmospheric muon neutrinos observed by Kamiokande. We find a small segment of the δm_{23}^2 vs. $\sin^2 2\theta_{23}$ plane exists where such solutions can be achieved and identify the class of righthanded Majorana submatrices required.

PACS numbers: 12.15.Ff, 14.60Gh, 14.80Dq, 96.60Kx

*Permanent address

†Electronic address: ALBRIGHT@FNAL

Operated by Universities Research Association Inc. under contract with the United States Department of Energy

Four important pieces of experimental information have emerged over the last five years which have a direct bearing on our understanding of neutrino physics, with deep implications for neutrino masses and mixings. The long-standing problem of the depletion of the solar electron-neutrino flux, as measured by Davis[1] in a tank of chlorene-rich liquid deep in the Homestake mine, has been confirmed by the Kamiokande deep mine experiment[2] with a water Cerenkov counter. Moreover, the theoretical explanation espoused by Mikheyev, Smirnov and Wolfenstein[3] (MSW) involving resonant oscillations by neutrinos traversing the dense solar matter is well demonstrated, provided the squared mass difference δm^2_{12} and mixing $\sin^2 2\theta_{12}$ lie along the nonadiabatic MSW band specified by[4]

$$\delta m^2_{12} \sin^2 \theta_{12} \simeq 10^{-8}\ \mathrm{eV}^2 \tag{1}$$

with $\delta m^2_{12} \lesssim 10^{-5}\ \mathrm{eV}^2$.

Two other results, namely the reemergence of a 17 keV neutrino coupled with strength $\sin^2 \theta \simeq 0.0085$ to the electron and the apparent depletion of atmospheric muon neutrinos relative to electron neutrinos, are more controversial. Solid-state detectors[5] implanted with ^{35}S, ^{3}H, ^{14}C and ^{71}Ge beta-decay sources appear to demonstrate evidence for a 17 keV neutrino signal 17 keV below the endpoint of the beta spectrum, while all spectrometer experiments[6] with similar sources observe no such evidence. The depletion of atmospheric muon neutrinos is seen in the Kamiokande and to some extent in the IMB experiments,[7] while the NUSEX and Frejus experiments[8] exhibit no such effect.

Finally, the very precise LEP experiments[9] have well documented that there are only three light families of $SU(2)_L \times U(1)_Y$ lefthanded flavor doublets. With the $\nu_e \leftrightarrow \nu_\mu$ oscillations accounting for the MSW effect, this leaves only the tau-neutrino flavor to which the 17 keV neutrino can contribute significantly on the one hand, and into which the atmospheric muon-neutrino can oscillate on the other. But for $\delta m^2_{23} = (17\mathrm{keV})^2$, the E531 experiment[10] at Fermilab has placed an upper bound of $\sin^2 2\theta_{23} < 0.004$, much too small to account for the atmospheric $\overset{(-)}{\nu}_\mu$ depletion.[7] Hence if both sets of controversial experiments which claim to see positive effects are to be interpreted as due to neutrino mixing and oscillation, they are in conflict experimentally.

Here we shall attempt a simultaneous explanation of the solar and atmospheric neutrino flux depletions, by foregoing the still-controversial 17 keV neutrino. Our model involves three lefthanded doublet neutrinos and three righthanded neutrino singlets in a standard grand-unified fashion exhibited by GUTs based on $SO(10)$, flipped $SU(5) \times U(1)$, E_6 and $SU(15)$, for example.[11] Unlike our previous attempt to incorporate the 17 keV neutrino,[12] here we meet with a fair measure of success and are able to display the appropriate neutrino mass matrix in some detail.

Our starting point, as stated in considerable detail in previous papers[13] labeled here (I) and (II), are the complex symmetric 6×6 mass matrices

$$M_N = \begin{pmatrix} 0 & \mathbf{M}_N \\ \mathbf{M}_N^T & \mathbf{R}_M \end{pmatrix}, \qquad M_L = \begin{pmatrix} 0 & \mathbf{M}_L \\ \mathbf{M}_L^T & 0 \end{pmatrix} \tag{2}$$

in the flavor bases $\overline{B_L} = \{\overline{\nu'_{iL}},\ \overline{(\nu_i'^c)_L}\}$, $B_R = \{(\nu_i'^c)_R,\ \nu'_{iR}\}$ for neutrinos and likewise for the charged leptons. Here $\mathbf{M}_N$ and $\mathbf{M}_L$ are the 3×3 Dirac mass submatrices which arise from Higgs doublets, while $\mathbf{R}_M$ is the 3×3 righthanded Majorana neutrino mass submatrix involving one or more Higgs singlets. No Higgs triplets are assumed present in the model.

In the spirit of grand unification, we assume forms for the Dirac submatrices which are analogous to the empirical matrices[14] deduced for the quarks on the basis of a top quark mass near 130 - 135 GeV favored by the neutral-current[15] and flavor-changing[16] data:

$$\mathbf{M}_N = \begin{pmatrix} 0 & A_N & A_N \\ A_N & A_N & B_N \\ A_N & B_N & C_N \end{pmatrix}, \qquad \mathbf{M}_L = \begin{pmatrix} 0 & iA'_L & -A'_L \\ -iA'_L & -A'_L & B'_L \\ -A'_L & B'_L & C'_L \end{pmatrix} \tag{3a}$$

The three charged-lepton parameters are determined uniquely from the known masses and invariant traces and determinant to be $A'_L = 7.576$ MeV, $B'_L = 0.4181$ GeV and $C'_L = 1.686$ GeV, while the neutrino entries are required to satisfy hierarchical chiral symmetry-breaking conditions[17] for which we assume the inequalities

$$0 < |A_N/C_N| \lesssim 0.2|B_N/C_N| \lesssim 0.04 \tag{3b}$$

The righthanded Majorana submatrix $\mathbf{R}_M$ remains completely unspecified without an explicit theoretical model. We shall assume here it is rank three, so as to give the well-known seesaw mechanism.[18]

We summarize briefly the procedure followed in (I) and (II). First consider only a diagonal $\mathbf{R}_M = \mathbf{D}_M = diag(D_1,\ D_2,\ D_3)$. From the scaling properties of the seesaw mechanism, if A_N, B_N and C_N are scaled by a factor of 10, while D_1, D_2 and D_3 are scaled by a factor of 100, the light masses and mixings remain unchanged; hence for this diagonal $\mathbf{R}_M$ situation, there are just 5 independent parameters: A_N/C_N, B_N/C_N and the three D_i/C_N's. The squares of the 6×3 mixing matrix elements $V_{\alpha j}$ in the mass basis, where $\alpha = 1-6$, $j = 1-3$, can be calculated from the mass matrices in (2) by a generalization of Jarlskog's projection operator technique[19] as explained fully in (I) and (II). In doing so, we find the value of $|V_{12}|^2$ is independent of the D_i's and determined only by the ratios A_N/C_N and B_N/C_N. A *minimum* value of $|V_{12}|$ exists such that $\sin^2 2\theta_{12} \sim 4|V_{12}|^2 \geq 0.0193$. This lower bound has interesting implications for the expected solar neutrino capture rates in the experimentally-preferred nonadiabatic MSW region which translates into a maximum capture rate in gallium of about 25 - 40 SNU in the nonadiabatic region, from the work[20] of Parke and Walker and Bahcall and Haxton as emphasized in (I). The preliminary data from the SAGE experiment[21] are quite consistent with this observation.

We now fix $|V_{12}|^2 \simeq \sin^2\theta_{12} = 0.00485$ and adjust $\delta m^2_{12} \equiv m^2_{\nu_2} - m^2_{\nu_1}$ so that the point lies in the narrow allowed nonadiabatic MSW band corresponding to Eq. (1), i.e., $\delta m^2_{12} \simeq 2.06 \times 10^{-6}$ eV^2. This is done by scaling the D_i's accordingly, where we chose D_i's in the ratios

$$10^4 : 10^2 : 1, \qquad 10^2 : 10 : 1, \qquad 1 : 1 : 1, \qquad 1 : 10 : 10^2, \qquad 1 : 10^2 : 10^4 \tag{4}$$

The allowed physical region in the δm^2_{23} vs. $\sin^2 2\theta_{23}$ plane is then bounded from below by the dot-dashed curve in Fig. 1, if one imposes the hierarchy conditions in (3b). For comparison, the present upper bounds from the E531 experiment[10] at Fermilab and the CDHSW[22] collaboration at CERN are indicated by the solid curves.

In (II) our analysis was generalized to include nondiagonal $\mathbf{R}_M$ by performing orthogonal rotations on the $\mathbf{D}_M$ forms used in (I). For this purpose, we selected the points in Fig. 1 indicated by crosses lying along curves for each of the cases in (4) above, and performed a Monte Carlo analysis by choosing at random 5000 rotations for each set of points. Fortunately, the values of $|V_{12}|^2$ remain fixed at 0.00485, while the D_i's must be rescaled with each rotation to maintain the same point in the MSW band at $\delta m^2_{12} = 2.06 \times 10^{-6}$ eV^2. The results appear in the form of the scatter plot also illustrated in Fig. 1. It is clear from this figure, that while the greater density of points indicating the largest probability lies within the dot-dashed curve obtained in (I), there are a number of exceptional points outside this boundary which can not be excluded on the basis of our analysis.

We now come to the main point of this paper and address the issue whether we can simultaneously explain not only the MSW depletion of the solar electron-neutrino flux but also the depletion of the atmospheric muon-neutrino flux. The Kamiokande[7] result, which appears to be the most positive todate, is quoted as

$$\frac{(\mu/e)_{data}}{(\mu/e)_{MC}} = 0.61 \pm 0.07 \tag{5a}$$

which we simply translate into the probability that the muon-flavor neutrino produced in the atmosphere by pion decay will remain a muon-flavor neutrino upon detection in the Kamiokande water Cerenkov counter:

$$0.54 \leq \mathrm{Prob}(\nu_\mu \rightarrow \nu_\mu) \leq 0.68 \tag{5b}$$

since the probability that the electron-neutrino remains an electron-neutrino is very close to unity. We shall approximate the three-component oscillation probability by

$$\begin{aligned} \mathrm{Prob}(\nu_\mu \rightarrow \nu_\mu) &= 1 - 4\textstyle\sum_{i<j=1}^{3}(V_{i\mu})^2(V_{j\mu})^2 \sin^2 \frac{\delta m_{ij}^2}{4E} L \\ &\simeq 1 - 2(V_{1\mu})^2(V_{3\mu})^2 - 2(V_{2\mu})^2(V_{3\mu})^2 \end{aligned} \tag{6}$$

since the 12 oscillation length is much longer than the atmospheric production flight-path length. In fact, detailed atmospheric neutrino flux calculations[23] suggest the 13 and 23 oscillations only become important for $\delta m_{13}^2 \sim \delta m_{23}^2 \gtrsim (0.1 - 2) \times 10^{-3}$ eV^2.

We now use (6) and impose the restriction (5b) on our results for the scatter plot obtained by the Euler rotations explained earlier. The points which survive this cut are indicated by the larger scatter points all located at the lower righthand edge of Fig. 1, below the CDHSW boundary curve and for $\sin^2 2\theta_{23} \gtrsim 0.65$. Of the 60,000 points generated by our Monte Carlo program, just slightly more than 100 pass the probability cut in (5b). Nevertheless, a scan through the mass and mixing output of the points selected shows a clear pattern, from which we can identify the form of $\mathbf{R}_M$ required.

The mixing matrices are all very similar, and in a special but typical case we find for the light 3×3 sector

$$|V_{\alpha j}|^2 = \begin{pmatrix} 0.99514 & 0.00485 & 0.00001 \\ 0.00367 & 0.76359 & 0.23274 \\ 0.00119 & 0.23156 & 0.76724 \end{pmatrix} \tag{7}$$

for which $\sin^2 2\theta_{23} = 0.711$, $\mathrm{Prob}(\nu_\mu \to \nu_\mu) = 0.64$; the two-component oscillation variable $\sin^2 2\theta_{12}$, determined from the formula for $\mathrm{Prob}(\nu_e \to \nu_e)$ analogous to (6) with all $\sin^2 \frac{\delta m^2_{ij}}{4E} L$ set equal to 0.5, is calculated to be $\sin^2 2\theta_{12} = 0.0194 = 4|V_{12}|^2$ as required. Note the unitary nature of this 3×3 submatrix which is an excellent check on our numerical procedure. The mass matrix parameters for this specific case are $A_N = 30$ MeV, $B_N = 10.8$ GeV and $C_N = 69.1$ GeV, when C_N is scaled relative to the charged lepton and quark mass matrices as noted in (I) and (II); with the righthanded Majorana mass submatrix then given by

$$\mathbf{R}_M = \begin{pmatrix} 0.0089 & 0.0103 & 0.0464 \\ 0.0103 & 0.0186 & 0.1174 \\ 0.0464 & 0.1174 & 0.8556 \end{pmatrix} \times 10^{15} \text{ GeV} \tag{8a}$$

the mass eigenvalues are found to be

$$\begin{aligned} &m_1 = 1.53 \times 10^{-11} \text{ eV}, \qquad &&m_2 = 1.44 \times 10^{-3} \text{ eV}, \qquad &&m_3 = 0.123 \text{ eV} \\ &m_4 = 8.74 \times 10^{10} \text{ GeV}, \qquad &&m_5 = 8.74 \times 10^{12} \text{ GeV}, \qquad &&m_6 = 8.74 \times 10^{14} \text{ GeV} \end{aligned} \tag{8b}$$

The class of models that simultaneously satisfies both the MSW effect for the solar defficiency and the depletion of the atmospheric ν_μ flux has the hierarchical chiral symmetry-breaking structure exhibited in (7) and more generally is proportional to the matrix

$$\mathbf{R}_M \sim \begin{pmatrix} \tan^2\beta\cos^2\gamma & -\tan^2\beta\sin\gamma\cos\gamma & -\tan\beta\cos\gamma \\ -\tan^2\beta\sin\gamma\cos\gamma & \tan^2\beta\sin^2\gamma & \tan\beta\sin\gamma \\ -\tan\beta\cos\gamma & \tan\beta\sin\gamma & 1 \end{pmatrix} \tag{9}$$

with $\beta \sim 9^o \pm 4^o$ and $\gamma \sim 90^o \pm 40^o$, where the Dirac submatrix is taken to have the hierarchy exhibited in (3).

In closing we point out that just several acceptable solutions with the simultaneous depletions were obtained when the point ($\sin^2\theta_{12} = 0.05$, $\delta m^2_{12} = 2.0 \times 10^{-7}$ eV^2) was chosen in the MSW band. It thus appears that the simultaneous depletion effect limits the allowed region in the nonadiabatic MSW band to the range between the two points (0.00485, 2.06×10^{-6} eV^2) and (0.05, 2.0×10^{-7} eV^2) for this class of models. It remains an interesting challenge to formulate a full Lagrangian theory which naturally gives the above structure for the neutrino mass matrix.

Remarks by Edward W. Kolb and Michael S. Turner concerning the relative merits of the 17 keV neutrino and the apparent depletion of the atmospheric muon-neutrino flux prompted this investigation. The author also acknowledges spirited conversations with Stephen J. Parke and the kind hospitality of the Fermilab Theoretical Physics Department. This research was supported in part by Grant No. PHY-8907806 from the National Science Foundation. Fermilab is operated by Universities Research Association, Inc. under contract with the United States Department of Energy.

References

[1] R. Davis et al., Phys. Rev. Lett. **20**, 1205 (1968); in *Neutrino '88*, ed. J. Schnepp et al. (World Scientific, 1988).

[2] K. Hirata et al., Phys. Rev. Lett. **65**, 1297, 1301 (1990).

[3] S. P. Mikheyev and A. Yu Smirnov, Sov. J. Nucl. Phys. **42**, 913 (1986); Sov. Phys. JETP **64**, 4 (1986); Nuovo Cimento **9C**, 17 (1986); L. Wolfenstein, Phys. Rev. D **17**, 2369 (1978); Phys. Rev. D **20**, 2634 (1979).

[4] E. W. Kolb, M. S. Turner and T. P. Walker, Phys. Lett. **175B**, 478 (1986); S. P. Rosen and S. M. Gelb, Phys. Rev. D **34**, 969 (1986); J. N. Bahcall and H. A. Bethe, Phys. Rev. Lett. **65**, 2233 (1990).

[5] J. J. Simpson, Phys. Rev. Lett. **54**, 1891 (1985); J. Simpson and A. Hime, Phys. Rev. D **39**, 1825 (1989); A. Hime and J. J. Simpson, Phys. Rev. D **39**, 1837 (1989); B. Sur et al., Phys. Rev. Lett. **66**, 2444 (1991); A. Hime and N. A. Jelley, Phys. Lett. B **257**, 441 (1991); I. Zlimen et al., Ruder Boskovic Institute preprint 11-9/90 LEI.

[6] Among the latest is H.-W. Becker et al., Caltech preprint CALT-63-605, and references therein.

[7] K. S. Hirata, et al., Phys. Lett. B **205**, 416 (1988); T. Kajita, in *Singapore '90*, (World Scientific); D. Casper et al., Phys. Rev. Lett. **66**, 2561 (1991).

[8] Ch. Berger et al., Phys. Lett. B **245**, 305 (1990); Phys. Lett. B **227**, 489 (1989); M. Aglietta et al., Europhys. Lett. **8**, 611 (1989).

[9] D. Decamp et al. (ALEPH Collab.), Phys. Lett. B **235**, 399 (1990); M. Z. Akrawy et al. (OPAL Collab.), Phys. Lett. B **240**, 497 (1990); P. Aarnio et al. (DELPHI

Collab.), Phys. Lett. B **241**, 425 (1990); B. Adeva et al. (L3 Collab.), Phys. Lett. B **249**, 341 (1990).

[10] N. Ushida et al., Phys. Rev. Lett. **57**, 2897 (1986).

[11] R. Johnson, S. Ranfone and J. Schechter, Phys. Lett. **179B**, 355 (1986); G. Lazarides and Q. Shafi, ICTP preprint IC-90-153; I. Antoniadis, J. Ellis, J. S. Hagelin and D. V. Nanopoulos, Phys. Lett.B **231**, 65 (1989); P. H. Frampton and B.-H. Lee, Phys. Rev. Lett. **64**, 619 (1990).

[12] C. H. Albright, Fermilab preprint FERMILAB-PUB-91/29-T, to be published.

[13] C. H. Albright, Phys. Rev. D **43**, R3595 (1991), henceforth referred to as (I); Fermilab preprint FERMILAB-PUB-91/182-T referred to as (II).

[14] C. H. Albright, Phys. Lett. B **246**, 451 (1990); Fermilab preprint FERMILAB-CONF-90/104-T submitted to the XXV International High Energy Physics Conference, Singapore (1990).

[15] J. Ellis and G. L. Fogli, Phys. Lett. B **232**, 139 (1989); P. Langacker, Phys. Rev. Lett. **63**, 1920 (1989); V. Barger, J. L. Hewett and T. G. Rizzo, Phys. Rev. Lett. **65**, 1313 (1990); J. L. Rosner, Phys. Rev. D **42**, 3107 (1990).

[16] Cf., eg., Fermilab preprint FERMILAB-CONF-90/196-T, to appear in Proceedings of the XXV Int. HEP Conf., Singapore (1990); and references therein.

[17] H. Fritzsch, Phys. Lett. **70B**, 436 (1977); **73B**, 317 (1978); **166B**, 423 (1986).

[18] M. Gell-Mann, P. Ramond and R. Slansky, in "Supersymmetry," edited by P. Van Nieuwenhuizen and D. Z. Freedman (North Holland, 1979); T. Yanagida, Prog. Theor. Phys. B **315**, 66 (1978).

[19] C. Jarlskog, Phys. Rev. D **35**, 1685 (1987); D **36**, 2138 (1987); C. Jarlskog and A. Kleppe, Nucl. Phys. B **286**, 245 (1987).

[20] S. J. Parke and T. P. Walker, Phys. Rev. Lett. **57**, 2322 (1986); J. N. Bahcall and W. C. Haxton, Phys. Rev. D **40**, 931 (1989).

[21] V. N. Gavrin, in Proceedings of the XXV International Conference on High Energy Physics, Singapore (1990).

[22] F. Dydak et al., Phys. Lett. B **134**, 281 (1984).

[23] S. Midorikawa, M. Honda and K. Kasahara, U. of Tokyo preprint ICRR-Report-243-91-12.

Figure Caption

Figure 1: Scatter plot in the δm^2_{23} vs. $\sin^2 2\theta_{23}$ plane obtained by rotating the diagonal $\mathbf{D}_M$ matrices in (4) through Euler angles chosen by 5000 sets of Monte Carlo throws for each point indicated by a cross. The solid curves represent the present experimental upper limits, while the dot-dashed curve represents the hierarchical lower bound obtained with the diagonal forms of (4). The special points corresponding to the simultaneous depletion solutions are represented by larger dots at the lower corner of the plot.

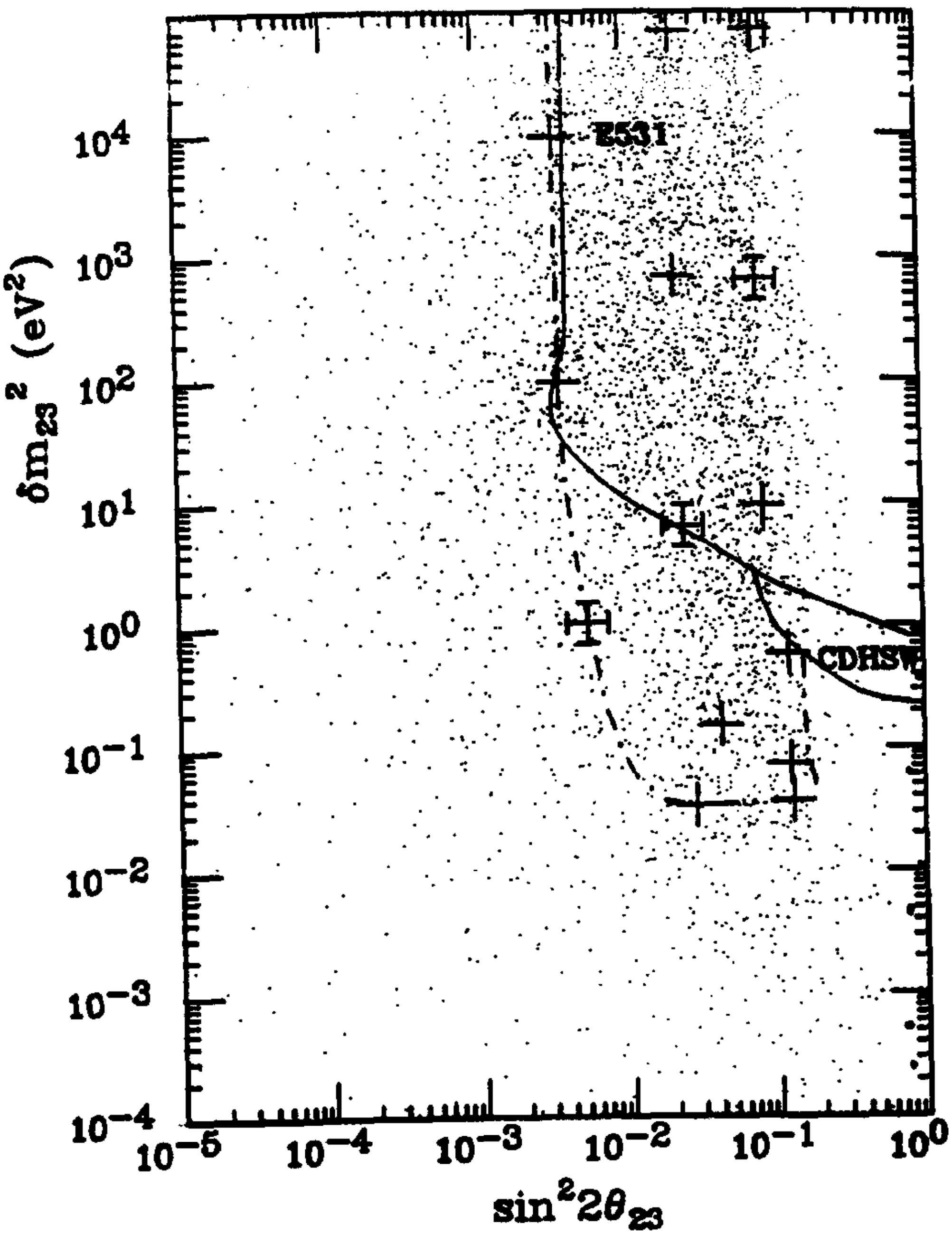

E531
CDHSW
10^4
10^3
10^2
10^1
10^0
10^{-1}
10^{-2}
10^{-3}
10^{-4}
$\delta m_{23}{}^2$ (eV^2)
10^{-5}
10^{-4}
10^{-3}
10^{-2}
10^{-1}
10^0
$\sin^2 2\theta_{23}$

Fig. 1